Koopmans' condition for density-functional theory

Ismaila Dabo,[1,*] Andrea Ferretti,[2,†] Nicolas Poilvert,[2] Yanli Li,[3] Nicola Marzari,[2,†] and Matteo Cococcioni[4]

[1]*CERMICS, Projet Micmac ENPC-INRIA, Université Paris-Est, 6-8 avenue Blaise Pascal, 77455 Marne-la-Vallée Cedex 2, France*
[2]*Department of Materials Science and Engineering, Massachusetts Institute of Technology, Cambridge, Massachusetts 02139, USA*
[3]*Department of Physics, Institute of Theoretical Physics and Astrophysics, and Fujian Key Laboratory of Semiconductor Materials and Applications, Xiamen University, Xiamen 361005, Republic of China*
[4]*Department of Chemical Engineering and Materials Science, University of Minnesota, Minneapolis, Minnesota 55455, USA*

In approximate Kohn-Sham density-functional theory, self-interaction manifests itself as the dependence of the energy of an orbital on its fractional occupation. This unphysical behavior translates into qualitative and quantitative errors that pervade many fundamental aspects of density-functional predictions. Here, we first examine self-interaction in terms of the discrepancy between total and partial electron removal energies, and then highlight the importance of imposing the generalized Koopmans' condition—that identifies orbital energies as opposite total electron removal energies—to resolve this discrepancy. In the process, we derive a correction to approximate functionals that, in the frozen-orbital approximation, eliminates the unphysical occupation dependence of orbital energies up to the third order in the single-particle densities. This non-Koopmans correction brings physical meaning to single-particle energies; when applied to common local or semilocal density functionals it provides results that are in excellent agreement with experimental data—with an accuracy comparable to that of GW many-body perturbation theory—while providing an explicit total energy functional that preserves or improves on the description of established structural properties.

PACS number(s): 31.15.E−, 32.10.Hq, 32.80.Fb, 33.15.Ry

I. INTRODUCTION

Density-functional approximations,[1] which account for correlated electron interactions via an explicit functional E_{xc} of the electronic density ρ, provide very good predictions of total energy differences for systems with nonfractional occupations.[2] One of the notable successes of local and semilocal density-functional calculations is the accurate description of ionization processes involving the complete filling or entire depletion of frontier orbitals. In quantitative terms, the local-spin-density (LSD) approximation and semilocal generalized-gradient approximations (GGAs) predict the energy differences of such reactions, namely, the electron affinity

$$A_N = E_N - E_{N+1} \qquad (1)$$

and the first ionization potential

$$I_N = E_{N-1} - E_N \qquad (2)$$

(where E_N stands for the ground-state energy of the N-electron system) with a precision of a few tenths of an electron volt, which compares favorably to that of more expensive wave function methods.[3]

Considering the excellent performance of density-functional approximations in predicting total ionization energies, it is surprising to discover that the same theories fail in describing partial ionization processes. As a matter of fact, local and semilocal functionals overestimate (by as much as 40%) the absolute energy difference per electron

$$\mathcal{A}_N = -\left.\frac{dE_M}{dM}\right|_{M=N^+} \qquad (3)$$

of an infinitesimal electron addition and underestimate with the same error differential energy changes

$$\mathcal{I}_N = -\left.\frac{dE_M}{dM}\right|_{M=N^-} \qquad (4)$$

upon electron removal.

Analytically, the discrepancy between total and partial differential ionization energies manifests itself into the convexity of E_N^{LSD} as a function of N (Fig. 1) while the exact ground-state energy E_N versus N is known to be described by a series of straight-line segments with positive derivative dis-
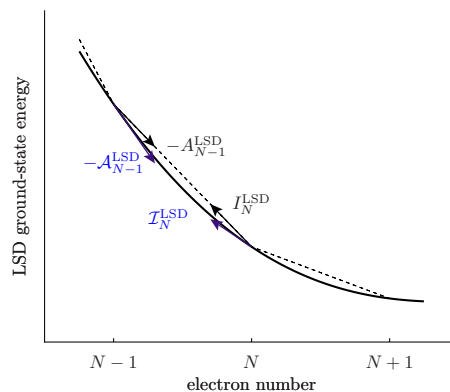

FIG. 1. (Color online) Convexity of the LSD ground-state energy as a function of the electron number, which results from the discrepancy between total and partial differential electron removal energies, i.e., $\mathcal{I}_N^{LSD} < I_N^{LSD} = A_{N-1}^{LSD} < \mathcal{A}_{N-1}^{LSD}$.

continuities at integer values of N.[4] (For simplicity, we restrict the entire discussion to the case of the LSD functional; semilocal GGA functionals exhibit identical trends.)

It is important to note that the discrepancy described above can be also related to the incorrect analytical behavior of the LSD chemical potential μ_N^{LSD}, i.e., the Lagrange multiplier associated to particle-number conservation in the near-zero temperature grand-canonical minimization of the total energy, $\min_\rho\{E[\rho]-\mu\int d\mathbf{r}\rho(\mathbf{r})\}$,[4–8] which can be interpreted physically as the opposite electronegativity of the system[5,6]

$$\mu_N = -\chi_N = -\frac{\mathcal{A}_N + \mathcal{I}_N}{2} \qquad (5)$$

and determines the direction and magnitude of electron transfer between separated molecular fragments.[4] In fact, the exact dependence of the chemical potential μ_N when N varies through an integer particle number Z is known to be

$$\mu_N = \begin{cases} -I_Z & Z-1 < N < Z \\ -\chi_Z^{\mathcal{M}} = -\frac{1}{2}(A_Z + I_Z) & N = Z \\ -A_Z & Z < N < Z+1, \end{cases} \qquad (6)$$

where $\chi_N^{\mathcal{M}}$ denotes the Mulliken electronegativity[9] of the N-electron system.[4,8]

In related physical terms, the discrepancy between ionization energies is often interpreted as arising from electron self-interaction that causes the removal of a small fraction of an electron from a filled electronic state to be energetically less costly, in absolute value, than its addition to the corresponding empty state.[10]

This self-interaction error is at the origin of important quantitative and qualitative failures that pervade crucial aspects of electronic-structure predictions.[11] Consider, for example, the dissociation of a cation dimer X_2^+ in the infinite interatomic separation limit. Here, the energy cost of removing a small electron fraction from X is lower than the energy gained in adding an electron fraction to X^+. As a result, a portion of the electronic charge will transfer from X to X^+, eventually leading to the split-charge configuration $2X^{1/2+}$, with a total energy that is correspondingly overstabilized with respect to the exact solution.

Related self-interaction artifacts explain other important failures of local and semilocal functionals in predicting electron-transfer processes,[12,13] electronic transport,[14] molecular adsorption,[15,16] reaction barriers and energies,[17–19] and electrical polarization in extended systems.[20–23] Self-interaction is also connected to the underestimation of the differential energy gap $\epsilon_{\text{gap}}^{\text{deriv}} = \mathcal{I}_N - \mathcal{A}_N$ of molecules, semiconductors, and insulators within LSD and GGAs.[24–28]

This work is organized as follows. First, we reexamine the Perdew-Zunger (PZ) one-electron self-interaction correction in terms of total and differential ionization energies. Then, after deriving an exact measure of the unphysical curvature of E_N as a function of N based on the generalized Koopmans' theorem, we introduce a functional that minimizes self-interaction errors by enforcing Koopmans' condition, thereby largely eliminating the discrepancy between total and differ-
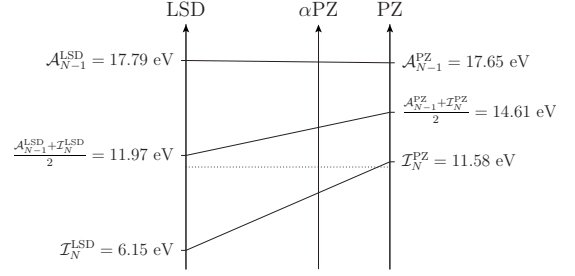

FIG. 2. LSD differential ionization energies $\mathcal{A}_{N-1}^{\text{LSD}}$, $\mathcal{I}_N^{\text{LSD}}$, and their arithmetic mean $\frac{1}{2}(\mathcal{A}_{N-1}^{\text{LSD}} + \mathcal{I}_N^{\text{LSD}})$ compared with PZ differential ionization energies for carbon. The dotted line indicates the position of the experimental ionization potential. The behavior of a PZ functional linearly downscaled by a factor α^{PZ} is also shown.

ential ionization energies while restoring the piecewise linearity of the ground-state energy. We conclude the study with extensive atomic and molecular calculations to demonstrate the predictive power of the non-Koopmans (NK) self-interaction correction.

II. SELF-INTERACTION CORRECTION

A. Perdew-Zunger one-electron correction

Several methods have been proposed to reduce self-interaction contributions and restore the internal consistency between total and partial electron removal energies.[13,26–38] A widely used approach is that introduced by Perdew and Zunger,[10] which consists of correcting self-interaction in the one-electron approximation by subtracting one-electron Hartree and exchange-correlation contributions. Explicitly, at the LSD level, the PZ orbital-dependent functional and Hamiltonian are defined as

$$E^{\text{PZ}} = E^{\text{LSD}} + \sum_{i\sigma} \left(-E_{\text{H}}[\rho_{i\sigma}] - E_{\text{xc}}[\rho_{i\sigma}] \right), \qquad (7)$$

$$= E^{\text{LSD}} + \sum_{i\sigma} \Xi_{i\sigma}, \qquad (8)$$

$$\hat{h}_{i\sigma}^{\text{PZ}} = \hat{h}^{\text{LSD}}[\rho] - \hat{v}_{\text{H}}[\rho_{i\sigma}] - \hat{v}_{\text{xc},\sigma}[\rho_{i\sigma}], \qquad (9)$$

where $\rho_{i\sigma}(\mathbf{r})$ denotes the orbital density ($\sigma = \pm\frac{1}{2}$ represents the spin), $v_{\text{H}}(\mathbf{r}) = \delta E_{\text{H}}/\delta\rho(\mathbf{r})$ is the electrostatic Hartree potential, $v_{\text{xc},\sigma}(\mathbf{r}) = \delta E_{\text{xc}}/\delta\rho_\sigma(\mathbf{r})$ stands for the spin-dependent exchange-correlation potential, and the PZ one-electron corrective contributions are defined as $\Xi_{i\sigma} = -E_{\text{H}}[\rho_{i\sigma}] - E_{\text{xc}}[\rho_{i\sigma}]$.

The effect of the PZ self-interaction correction on the partial electron removal energies of an isolated carbon atom is depicted in Fig. 2. We observe that the LSD differential ionization potential $\mathcal{I}_N^{\text{LSD}}$ and electron affinity $\mathcal{A}_{N-1}^{\text{LSD}}$ deviate by more than 5 eV from the experimental total removal energy, whereas their average is in close agreement with experiment. The PZ correction improves the precision of the predicted ionization potential $\mathcal{I}_N^{\text{PZ}}$, reducing the error to less than 0.4 eV. The inaccuracy of the PZ electron affinity $\mathcal{A}_{N-1}^{\text{PZ}}$ remains almost unchanged due to the fact that the PZ one-electron correction vanishes for empty states (the slight variation of

the differential electron affinity from 17.79 to 17.65 eV is only due to the self-consistent reconfiguration of the occupied manifold). Consequently, the PZ functional achieves a substantial but only partial correction of self-interaction, reducing the unphysical convexity, i.e., the discrepancy $\mathcal{A}_{N-1} - \mathcal{I}_N$, by a factor of two.

Another notable feature in Fig. 2 is the overestimation of the average of the ionization potential $\mathcal{I}_N^{PZ}$ and electron affinity $\mathcal{A}_{N-1}^{PZ}$. Since the average $\frac{1}{2}(\mathcal{A}_{N-1}^{PZ} + \mathcal{I}_N^{PZ})$ roughly approximates I_N^{PZ},[10,39] this deviation translates into overestimated total ionization energies and excessively negative ground-state energies $E_N^{PZ} = -\Sigma_{M=1}^{N} I_M^{PZ}$. (Semiempirical relations between total energies and low-order ionization potentials have been also evidenced by Pucci and March in Ref. 40.) In the case of isolated atoms, the energy underestimation improves on the description of electron correlation, bringing PZ ground-state energies in remarkable agreement with experiment.[10] However, in the more general case of many-electron polyatomic systems, PZ ground-state energies are found to be overcorrelated, yielding inaccurate dissociation energies and excessively short bond lengths.[41]

Various downscaling methods have been proposed to correct the above trends. Nevertheless, the performance of such schemes is inherently limited by the fact that downscaling the PZ correction impairs the accuracy of differential ionization energies. For example, it is seen in Fig. 2 that a functional $E^{\alpha PZ}$, in which the self-interaction correction is linearly downscaled by a factor α^{PZ}

$$E^{\alpha PZ} = E^{LSD} + \alpha^{PZ}(E^{PZ} - E^{LSD}) \qquad (10)$$

cannot counterbalance the deviation of $I_N^{PZ} \approx \frac{1}{2}(\mathcal{A}_{N-1}^{PZ} + \mathcal{I}_N^{PZ})$ without altering the precision of $\mathcal{I}_N^{PZ}$. More sophisticated downscaling methods exhibit identical trends.[32,42–44]

In the next sections, we will derive a correction that cancels self-interaction errors for systems with fractional occupations without affecting the precision of total energy differences and equilibrium structural properties for systems with nonfractional occupations.

B. Measure of self-interaction

The initial conceptual step in the construction of the self-interaction correction is to set forth a quantitative measure of self-interaction errors valid in the many-electron case—i.e., beyond the one-electron approximation of the Perdew-Zunger correction. With this self-interaction measure in hand, we will construct an improved self-interaction correction functional, working first in the simplified picture where electronic orbitals are kept frozen (Sec. II C), and then considering orbital relaxation as the next stage of refinement (Sec. II E).

Before doing so, to derive this measure, we start from the physical intuition that self-interaction relates to the unphysical variation of the energy of an orbital $\epsilon_{i\sigma}(f)$ as a function of its own occupation f. Hence, a *necessary* nonself-interaction condition can be written as

$$\left. \frac{d\epsilon_{i\sigma}(f')}{df'} \right|_{f'=f} = 0, \quad 0 \le f \le 1. \qquad (11)$$

(Here, f stands for a variable occupation while $f_{i\sigma}$ denotes the orbital occupation that enters into the expression of the total energy functional.) Invoking Janak's theorem,[45] this necessary condition on orbital-energy derivatives can be restated as a criterion on the curvature of the total energy

$$\left. \frac{d^2 E_{i\sigma}(f')}{df'^2} \right|_{f'=f} = 0, \quad 0 \le f \le 1, \qquad (12)$$

where $E_{i\sigma}(f)$ is the total energy E minimized under the constraint $f_{i\sigma} = f$ (leaving all other occupations unchanged). Thus, in the absence of self-interaction, the total energy does not display any curvature upon varying occupations. As a corollary, any self-interaction-free functional satisfies the linearity condition

$$\Delta E_{i\sigma} = -f_{ic} \left. \frac{dE_{i\sigma}(f')}{df'} \right|_{f'=f}, \quad 0 \le f \le 1, \qquad (13)$$

where

$$\Delta E_{i\sigma} = E_{i\sigma}(0) - E_{i\sigma}(f_{i\sigma}) \qquad (14)$$

denotes the removal energy of the orbital $\psi_{i\sigma}$.[11,44,46]

Invoking once more Janak's theorem, the above nonself-interaction condition yields the *generalized Koopmans' theorem*

$$\Delta E_{i\sigma} = -f_{i\sigma}\epsilon_{i\sigma}(f), \quad 0 \le f \le 1 \qquad (15)$$

(The equivalence between Eq. (11) and Eq. (15) highlights the significance of Koopmans' theorem for the quantitative assessment of self-interaction.) It is then convenient to measure self-interaction in terms of the energies $\Pi_{i\sigma}$ first introduced by Perdew and Zunger (see Sec. II D in Ref. 10) in analyzing discrepancies between orbital energies and vertical ionization energies[47]

$$\Pi_{i\sigma}(f) = f_{i\sigma}\epsilon_{i\sigma}(f) + \Delta E_{i\sigma}. \qquad (16)$$

Because the self-interaction energies $\Pi_{i\sigma}$ quantify deviations from the Koopmans' linearity [Eq. (15)], they will be termed here *non-Koopmans energies*—the same terminology as that employed in Ref. 10 and 37.

Making then use of Slater's theorem[48]

$$\Delta E_{i\sigma} = -\int_0^{f_{i\sigma}} df \epsilon_{i\sigma}(f) \qquad (17)$$

the non-Koopmans energy can be rewritten as

$$\Pi_{i\sigma}(f) = \int_0^{f_{i\sigma}} df'[\epsilon_{i\sigma}(f) - \epsilon_{i\sigma}(f')]. \qquad (18)$$

In this form, the energy $\Pi_{i\sigma}(f)$ is clearly seen to correspond to the integrated change of the orbital energy upon varying the orbital occupation—in particular, it is straightforward to verify that $\Pi_{i\sigma}(f) = 0$ if the orbital energy $\epsilon_{i\sigma}(f')$ does not vary with the orbital occupation f'.

Using the measure defined in Eq. (16), the nonself-

interaction criterion [Eq. (11)] can be restated exactly as a *generalized Koopmans' condition*

$$\Pi_{i\sigma}(f) = 0, \quad 0 \le f \le 1. \tag{19}$$

Equation (19) is of central importance in this work; it provides a simple quantitative criterion in terms of a rigorous nonlinearity measure to assess and correct self-interaction errors. The suggestion of using non-Koopmans corrections to minimize self-interaction has been recently introduced, in preliminary form, by Dabo, Cococcioni, and Marzari in Ref. 49, and, in heuristic form, by Lany and Zunger in Ref. 36. In the context of range-separated hybrid functionals, the importance of satisfying Koopmans' equalities for frontier molecular orbitals has also been evidenced by Stein, Kronik and Baer in Ref. 13. The consequences of Koopmans' condition are discussed in the next sections.

C. Bare non-Koopmans correction

On the basis of the above quantitative analysis, our objective now is to linearize the dependence of the total energy as a function of orbital occupations by modifying the expression of the energy functional in order to cancel the non-Koopmans terms $\Pi_{i\sigma}(f)$. To render this complex problem tractable, we first consider the restricted case where all orbitals are frozen while the occupation of one of them is changing in the course of a fictitious ionization process (the frozen-orbital approximation). Within this paradigm, Eq. (19) becomes the *restricted Koopmans' condition*

$$\Pi^u_{i\sigma}(f) = 0, \quad 0 \le f \le 1, \tag{20}$$

where the superscript *u* stands for *unrelaxed*. Here, the frozen-orbital non-Koopmans energy $\Pi^u_{i\sigma}$ is defined as

$$\Pi^u_{i\sigma}(f) = \int_0^{f_{i\sigma}} df' [\epsilon^u_{i\sigma}(f) - \epsilon^u_{i\sigma}(f')], \tag{21}$$

where $\epsilon^u_{i\sigma}(f)$ is the unrelaxed orbital energy calculated keeping all the orbitals frozen while setting $f_{i\sigma}$ to be f. We underscore that in the specific case of one-electron systems and for $f=0$, Eq. (20) yields the one-electron self-interaction condition of Perdew and Zunger[10]

$$\Xi_{i\sigma} = 0. \tag{22}$$

The restricted Koopmans' condition is thus seen to encompass the Perdew-Zunger condition, thereby representing a more comprehensive criterion for assessing and correcting self-interaction errors.

Expectedly, satisfying the restricted Koopmans' condition is exactly equivalent to fulfilling the restricted Koopmans' theorem

$$\Delta E^u_{i\sigma} = -f_{i\sigma}\epsilon^u_{i\sigma}(f), \quad 0 \le f \le 1, \tag{23}$$

where

$$\Delta E^u_{i\sigma} = E^u_{i\sigma}(0) - E^u_{i\sigma}(f_{i\sigma}) \tag{24}$$

denotes the unrelaxed electron removal energy.

An example of a functional that exhibits a linear frozen-orbital energy dependence is provided by the Hartree-Fock

(HF) theory, generalized to fractional occupations. Indeed, at the HF level, one can verify that

$$\Pi^{u,\mathrm{HF}}_{i\sigma}(f) = 0, \quad 0 \le f \le 1 \tag{25}$$

due to the fact that the expectation value $\epsilon^{u,\mathrm{HF}}_{i\sigma}(f)$ does not depend on f.

For functionals that do not satisfy the restricted Koopmans' condition [Eq. (20)], the unrelaxed electron removal energy can only be expressed in terms of the restricted Slater integral

$$\Delta E^u_{i\sigma} = -\int_0^{f_{i\sigma}} df\, \epsilon^u_{i\sigma}(f) \tag{26}$$

(note that this relation is satisfied by any functional whether it is subject or not to self-interaction errors).

These considerations allow us to introduce our corrected functional aiming to satisfy Koopmans' condition; at frozen orbital, it is obtained by replacing Slater terms—Eq. (26), where single-particle energies are function of their own occupation—with Koopmans terms—Eq. (23), where single-particle energies do not depend on occupations. In particular, we evaluate here the Koopmans terms at a given orbital occupation $f=f_\mathrm{ref}$ that defines the reference transition state (the determination of the reference occupation f_ref shall be explained on the basis of Slater's approximation and exchange-correlation hole arguments in Sec. II F). Explicitly, in the case of the LSD functional, the NK self-interaction correction to the energy is defined as

$$E^\mathrm{NK} = E^\mathrm{LSD} - \sum_{i\sigma} \left[-f_{i\sigma}\epsilon^{u,\mathrm{LSD}}_{i\sigma}(f_\mathrm{ref}) + \int_0^{f_{i\sigma}} df\, \epsilon^{u,\mathrm{LSD}}_{i\sigma}(f) \right], \tag{27}$$

where the negative sign in front of the sum follows from the convention that ionization energies are positive. Rewriting Eq. (27) in terms of the frozen-orbital non-Koopmans energies of Eq. (21), we obtain

$$E^\mathrm{NK} = E^\mathrm{LSD} + \sum_{i\sigma} \Pi^{u,\mathrm{LSD}}_{i\sigma}(f_\mathrm{ref}), \tag{28}$$

where the non-Koopmans corrective terms can now be recast into the explicit functional form

$$\Pi^{u,\mathrm{LSD}}_{i\sigma}(f_\mathrm{ref}) = f_{i\sigma}(2f_\mathrm{ref} - f_{i\sigma})E_\mathrm{H}[n_{i\sigma}] - E^\mathrm{LSD}_\mathrm{xc}[\rho] $$
$$+ E^\mathrm{LSD}_\mathrm{xc}[\rho - \rho_{i\sigma}] + \int d\mathbf{r}\rho_{i\sigma}(\mathbf{r})v^\mathrm{LSD}_{\mathrm{xc},\sigma}(\mathbf{r};[\rho^\mathrm{ref}_{i\sigma}])d\mathbf{r}, \tag{29}$$

where $n_{i\sigma}(\mathbf{r}) = |\psi_{i\sigma}|^2(\mathbf{r})$ and $\rho_{i\sigma}(\mathbf{r}) = f_{i\sigma}n_{i\sigma}(\mathbf{r})$. Here, the electronic density $\rho^\mathrm{ref}_{i\sigma}(\mathbf{r})$ stands for the reference transition-state density

$$\rho^\mathrm{ref}_{i\sigma}(\mathbf{r}) = f_\mathrm{ref}n_{i\sigma}(\mathbf{r}) + \sum_{j\sigma' \ne i\sigma} f_{j\sigma'}n_{j\sigma'}(\mathbf{r}), \tag{30}$$

$$= \rho(\mathbf{r}) + (f_\mathrm{ref} - f_{i\sigma})n_{i\sigma}(\mathbf{r}). \tag{31}$$

We now derive the expression of the orbital-dependent NK Hamiltonian. To this end, we first calculate the functional

derivative of the energy contribution $\Pi_{i\sigma}^{u,\mathrm{LSD}}(f_{\mathrm{ref}})$ with respect to variations of the orbital density $\rho_{i\sigma}$. The expression of the functional derivative reads

$$\frac{\delta \Pi_{i\sigma}^{u,\mathrm{LSD}}}{\delta \rho_{i\sigma}(\mathbf{r})} = (f_{\mathrm{ref}} - f_{i\sigma}) v_{\mathrm{H}}(\mathbf{r};[n_{i\sigma}]) + v_{\mathrm{xc},\sigma}^{\mathrm{LSD}}(\mathbf{r};[\rho_{i\sigma}^{\mathrm{ref}}])$$
$$- v_{\mathrm{xc},\sigma}^{\mathrm{LSD}}(\mathbf{r};[\rho]) + w_{\mathrm{ref},i\sigma}^{\mathrm{LSD}}(\mathbf{r}). \quad (32)$$

In Eq. (32), the potential $w_{\mathrm{ref},i\sigma}^{\mathrm{LSD}}$ denotes

$$w_{\mathrm{ref},i\sigma}^{\mathrm{LSD}}(\mathbf{r}) = f_{\mathrm{ref}}\Bigg[\int d\mathbf{r}' f_{\mathrm{Hxc},\sigma\sigma}^{\mathrm{LSD}}(\mathbf{r},\mathbf{r}';[\rho_{i\sigma}^{\mathrm{ref}}]) n_{i\sigma}(\mathbf{r}')$$
$$- \int d\mathbf{r}' d\mathbf{r}'' f_{\mathrm{Hxc},\sigma\sigma}^{\mathrm{LSD}}(\mathbf{r}',\mathbf{r}'';[\rho_{i\sigma}^{\mathrm{ref}}]) n_{i\sigma}(\mathbf{r}') n_{i\sigma}(\mathbf{r}'') \Bigg], \quad (33)$$

where $f_{\mathrm{Hxc},\sigma\sigma'}^{\mathrm{LSD}}(\mathbf{r},\mathbf{r}') = \delta^2(E_{\mathrm{H}} + E_{\mathrm{xc}}^{\mathrm{LSD}})/\delta \rho_\sigma(\mathbf{r}) \delta \rho_{\sigma'}(\mathbf{r}')$ is the second-order functional derivative of the LSD interaction energy.[50] Focusing then on the cross derivatives, we obtain

$$\frac{\delta \Pi_{j\sigma'}^{u,\mathrm{LSD}}}{\delta \rho_{i\sigma}(\mathbf{r})} = v_{\mathrm{xc},\sigma}^{\mathrm{LSD}}(\mathbf{r};[\rho - \rho_{j\sigma'}]) - v_{\mathrm{xc},\sigma}^{\mathrm{LSD}}(\mathbf{r};[\rho])$$
$$+ \int d\mathbf{r}' f_{\mathrm{xc},\sigma\sigma'}^{\mathrm{LSD}}(\mathbf{r},\mathbf{r}';[\rho_{j\sigma'}^{\mathrm{ref}}]) \rho_{j\sigma'}(\mathbf{r}'), \quad (34)$$

where $f_{\mathrm{xc},\sigma\sigma'}^{\mathrm{LSD}}(\mathbf{r},\mathbf{r}')$ is the exchange-correlation contribution to $f_{\mathrm{Hxc},\sigma\sigma'}^{\mathrm{LSD}}(\mathbf{r},\mathbf{r}')$. As a final result, the orbital-dependent NK Hamiltonian can be cast into the form

$$\hat{h}_{i\sigma}^{\mathrm{NK}} = \hat{h}^{\mathrm{LSD}}[\rho_{i\sigma}^{\mathrm{ref}}] + \hat{w}_{\mathrm{ref},i\sigma}^{\mathrm{LSD}} + \hat{w}_{\mathrm{xd},i\sigma}^{\mathrm{LSD}}, \quad (35)$$

where $w_{\mathrm{xd},i\sigma}^{\mathrm{LSD}}$ stands for the cross-derivative potential

$$w_{\mathrm{xd},i\sigma}^{\mathrm{LSD}}(\mathbf{r}) = \sum_{j\sigma' \neq i\sigma} \frac{\delta \Pi_{j\sigma'}^{u,\mathrm{LSD}}}{\delta \rho_{i\sigma}(\mathbf{r})}. \quad (36)$$

In a nutshell, the NK Hamiltonian consists of the uncorrected LSD Hamiltonian calculated at the reference density $\hat{h}^{\mathrm{LSD}}[\rho_{i\sigma}^{\mathrm{ref}}]$ with the addition of two variational potentials. The first additional term $\hat{w}_{\mathrm{ref},i\sigma}^{\mathrm{LSD}}$ results from the variation of the reference density as a function of $\rho_{i\sigma}$ while the second term $\hat{w}_{\mathrm{xd},i\sigma}^{\mathrm{LSD}}$ springs from the cross dependence of the non-Koopmans corrective terms. The effect of the $\hat{w}_{\mathrm{ref},i\sigma}^{\mathrm{LSD}}$ and $\hat{w}_{\mathrm{xd},i\sigma}^{\mathrm{LSD}}$ contributions that arise as byproducts of variationality is analyzed in the next section.

D. Comparative assessment

In this section, we assess the performance of the NK self-interaction correction, particularly focusing on the effect of variational terms on the accuracy of NK orbital predictions—i.e., on the cancellation of the unrelaxed frozen-orbital self-interaction measure $\Pi_{i\sigma}^{u,\mathrm{NK}}(f)$. One simple and probably the most direct way to evaluate the influence of $\hat{w}_{\mathrm{ref},i\sigma}^{\mathrm{LSD}}$ and $\hat{w}_{\mathrm{xd},i\sigma}^{\mathrm{LSD}}$ is to introduce a nonvariational orbital-energy scheme, the NK_0 method, that consists of freezing the dependence of the reference transition-state densities and the
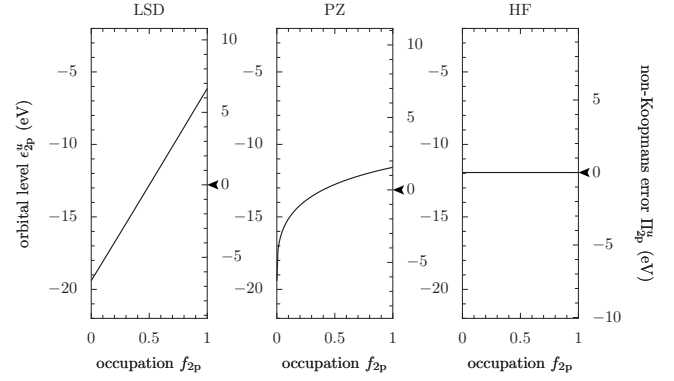

FIG. 3. LSD, PZ, and HF unrelaxed orbital energies and residual unrelaxed non-Koopmans errors of the highest occupied state of carbon. The black arrow highlights the zero value for the non-Koopmans error scale.

cross dependence of corrective energy terms, thereby eliminating $\hat{w}_{\mathrm{ref},i\sigma}^{\mathrm{LSD}}$ and $\hat{w}_{\mathrm{xd},i\sigma}^{\mathrm{LSD}}$ contributions to the effective potential. Computed NK and NK_0 orbital levels can then be compared for the direct assessment of $\hat{w}_{\mathrm{ref},i\sigma}^{\mathrm{LSD}}$ and $\hat{w}_{\mathrm{xd},i\sigma}^{\mathrm{LSD}}$ errors. Explicitly, the NK_0 Hamiltonian can be written as

$$\hat{h}_{i\sigma}^{\mathrm{NK}_0} = \hat{h}^{\mathrm{LSD}}[\rho] + \frac{\delta \Pi_{i\sigma}^{u,\mathrm{LSD}}}{\delta \hat{\rho}_{i\sigma}} \Bigg|_{\rho_{i\sigma}^{\mathrm{ref}}=\mathrm{cst}}, \quad (37)$$

$$\hat{h}_{i\sigma}^{\mathrm{NK}_0} = \hat{h}^{\mathrm{LSD}}[\rho_{i\sigma}^{\mathrm{ref}}]. \quad (38)$$

In the NK_0 optimization scheme, the Hamiltonian given by Eq. (38) is employed to propagate orbital degrees of freedom at fixed $\rho_{i\sigma}^{\mathrm{ref}}$. Reference transition-state densities are then updated according to Eq. (30). The procedure is iterated until self-consistency.

Due to the loss of variationality, the obvious practical limitation of the nonvariational NK_0 orbital-energy method is that it cannot provide total energies and interatomic forces. However, NK_0 is of great utility in evaluating the intrinsic performance of the NK correction. In itself, the NK_0 formulation is also useful in determining orbital energy properties that are particularly affected by $\hat{w}_{\mathrm{ref},i\sigma}^{\mathrm{LSD}}$ and $\hat{w}_{\mathrm{xd},i\sigma}^{\mathrm{LSD}}$ errors.

Focusing now on computational predictions, the occupation dependencies of the LSD, HF, PZ, and NK unrelaxed orbital energies

$$\epsilon_{i\sigma}^{u}(f) = \frac{dE_{i\sigma}^{u}(f')}{df'} \Bigg|_{f'=f} \quad (39)$$

of the highest atomic orbital of carbon are depicted in Figs. 3 and 4(a). The salient feature of the LSD graph is the large variation of the orbital energy from -19.40 to -6.15 eV, reflecting the strong nonlinearity of the corresponding unrelaxed ionization curve. The PZ variation is found to be twice lower than for LSD, confirming the trends observed in Sec. II A. In contrast, the HF unrelaxed ionization curve exhibits a perfectly linear behavior (i.e., the unrelaxed orbital energy remains constant). This trend is closely reproduced by the NK functional [Fig. 4(a)]; on the scale of LSD residual non-Koopmans errors, the eye can barely distinguish any devia-
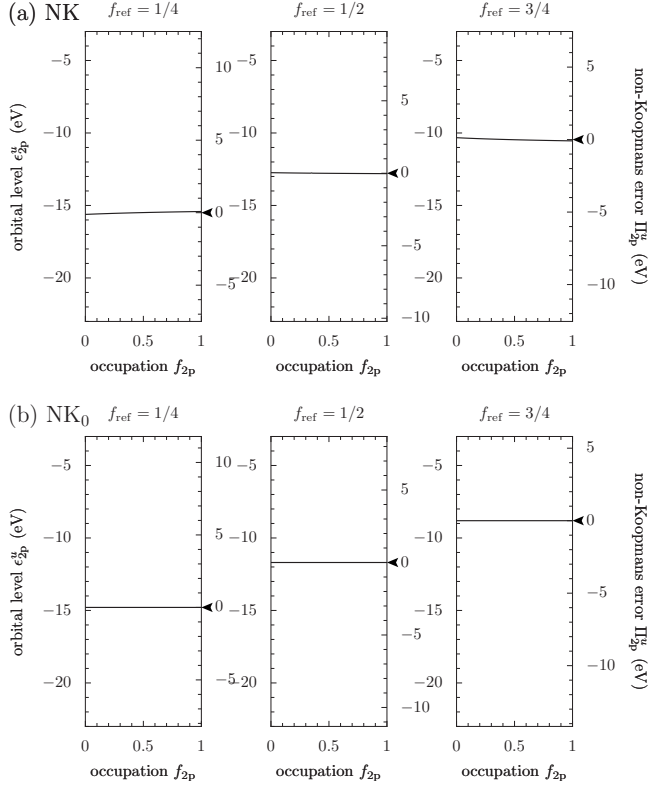
FIG. 4. Non-Koopmans unrelaxed orbital energies and residual unrelaxed non-Koopmans errors of the highest occupied state of carbon for select arbitrary values of the reference occupation ($f_{\mathrm{ref}} = \frac{1}{4}$, $\frac{1}{2}$, and $\frac{3}{4}$) using (a) the NK total-energy method and (b) the NK$_0$ orbital-energy method. The black arrow highlights the zero value for the non-Koopmans error scale.

tion of the NK unrelaxed orbital energies as a function of $f_{i\sigma}$ regardless of the value of the reference occupation.

The above observation is due to the fact that the variational contribution $\hat{w}_{\mathrm{ref},i\sigma}^{\mathrm{LSD}}$ affects the orbital energy $\epsilon_{i\sigma}^{\mathrm{NK}}$ indirectly, i.e., only through the self-consistent response of the orbital densities since $\langle \psi_{i\sigma} | \hat{w}_{\mathrm{ref},i\sigma}^{\mathrm{LSD}} | \psi_{i\sigma} \rangle = 0$ at self-consistency. Furthermore, a Taylor series expansion of $\hat{w}_{\mathrm{xd},i\sigma}^{\mathrm{LSD}}$ reveals that $\langle \psi_{i\sigma} | \hat{w}_{\mathrm{xd},i\sigma}^{\mathrm{LSD}} | \psi_{i\sigma} \rangle$ does not cause notable departure from the linear Koopmans' behavior. In quantitative terms, the dominant term in the expansion of the residual NK self-interaction error is of the fourth order in orbital densities

$$\Pi_{i\sigma}^{u,\mathrm{NK}}(f) = \frac{1}{4} \sum_{j\sigma' \neq i\sigma} f_{j\sigma'}(2f_{\mathrm{ref}} - f_{j\sigma'})(2f - f_{i\sigma})f_{i\sigma}$$

$$\times \int d\mathbf{r}_{1234} f_{\mathrm{xc},\sigma\sigma'\sigma'\sigma}^{(4),\mathrm{LSD}}(\mathbf{r}_{1234}; [\rho_{j\sigma'}^{\mathrm{ref}}])$$

$$\times n_{i\sigma}(\mathbf{r}_1)n_{j\sigma'}(\mathbf{r}_2)n_{j\sigma'}(\mathbf{r}_3)n_{i\sigma}(\mathbf{r}_4) + \cdots \quad (40)$$

(where $f_{\mathrm{xc},\sigma_{12\cdots n}}^{(n),\mathrm{LSD}}(\mathbf{r}_{12\cdots n})$ denotes the nth order functional derivative of the LSD exchange-correlation energy), whereas the PZ correction is found to be less accurate in minimizing the self-interaction measure by one order of precision
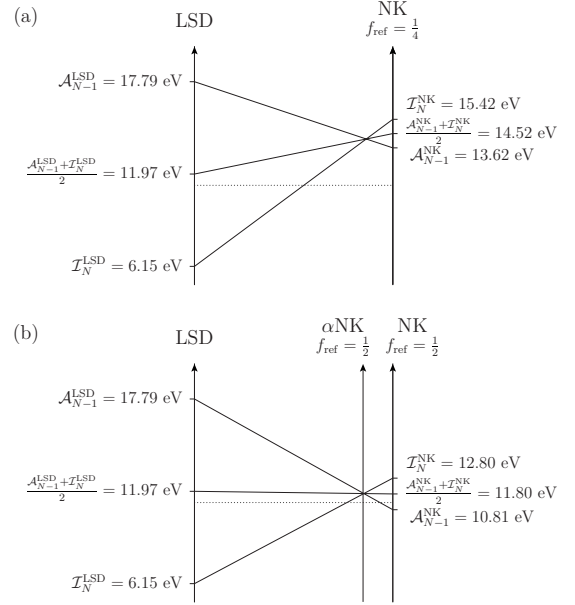

FIG. 5. LSD differential ionization energies $\mathcal{A}_{N-1}^{\mathrm{LSD}}$, $\mathcal{I}_N^{\mathrm{LSD}}$, and their average $\frac{1}{2}(\mathcal{A}_{N-1}^{\mathrm{LSD}} + \mathcal{I}_N^{\mathrm{LSD}})$ compared with NK differential ionization energies for (a) $f_{\mathrm{ref}} = \frac{1}{4}$ and (b) $f_{\mathrm{ref}} = \frac{1}{2}$ for carbon.

$$\Pi_{i\sigma}^{u,\mathrm{PZ}}(f) = \frac{1}{2} \sum_{j \neq i} (2f - f_{i\sigma})f_{i\sigma}f_{j\sigma} \int d\mathbf{r}_{123}$$

$$\times f_{\mathrm{xc},\sigma\sigma\sigma}^{(3),\mathrm{LSD}}(\mathbf{r}_{123}; [\rho - \rho_{i\sigma}])n_{i\sigma}(\mathbf{r}_1)n_{i\sigma}(\mathbf{r}_2)n_{j\sigma}(\mathbf{r}_3)$$

$$+ \cdots. \quad (41)$$

Despite the very good accuracy of the NK correction, direct confrontation with NK$_0$ results—for which the non-Koopmans measure $\Pi_{i\sigma}^{u,\mathrm{NK}_0}(f)$ [Eq. (21)] is obviously canceled for any value of f—reveals that NK tends to underestimate orbital energies with deviations of 0.5–1.5 eV that gradually increase with f_{ref} [Figs. 4(a) and 4(b)]. The practical consequences of this observation will be discussed in Sec. III.

As a conclusion of this preliminary performance evaluation, the NK frozen-orbital correction results in a considerable reduction of residual errors $\Pi_{i\sigma}^{u,\mathrm{NK}}(f)$, bringing density-functional approximations in nearly exact agreement with the frozen-orbital linear trend while exhibiting a slight tendency to underestimate orbital energies. In the next sections, we present an extension of the NK correction beyond the frozen-orbital paradigm.

E. Screened non-Koopmans correction

Having derived and examined the bare non-Koopmans frozen-orbital correction, we now turn to the analysis of self-interaction for relaxed orbitals. The effect of the NK correction on relaxed partial ionization energies for carbon is illustrated in Fig. 5. The first important observation is that the NK correction decreases the unphysical convexity of E_N, reducing the unphysical discrepancy $(\mathcal{A}_{N-1} - \mathcal{I}_N)$ by a factor of 6 regardless of the reference occupation f_{ref}.

The second notable feature is the fact that the NK correction reverts the convexity trend (i.e., $\mathcal{I}_N^{\mathrm{NK}} > \mathcal{A}_{N-1}^{\mathrm{NK}}$), transform-

ing the convex dependence of E_N into a piecewise concave curve. In fact, bearing in mind that relaxation contributions to E_N are always negative, it is relatively straightforward to show that any functional that satisfies the restricted Koopmans' condition [Eq. (20)] is piecewise concave. Consequently, in contrast to the αPZ functional introduced in Sec. II A, there always exists a value of the coefficient α^{NK} ($0 \leq \alpha^{NK} \leq 1$) for which the αNK functional

$$E^{\alpha NK} = E^{LSD} + \alpha^{NK}(E^{NK} - E^{LSD}) \qquad (42)$$

restores the agreement between $\mathcal{A}_{N-1}^{\alpha NK}$ and $\mathcal{I}_N^{\alpha NK}$. At this crossing point, the αNK relaxed ionization curve is in close agreement with the exact linear trend described by the generalized Koopmans' condition (see Sec. III A).

Making the approximation that ionization energies vary linearly with α^{NK}, the value of the coefficient for which the crossing $\mathcal{A}_{N-1}^{\alpha NK} = \mathcal{I}_N^{\alpha NK}$ occurs can be estimated as

$$\alpha^{NK} \approx \frac{\mathcal{A}_{N-1}^{LSD} - \mathcal{I}_N^{LSD}}{(\mathcal{A}_{N-1}^{LSD} - \mathcal{I}_N^{LSD}) - (\mathcal{A}_{N-1}^{NK} - \mathcal{I}_N^{NK})}. \qquad (43)$$

This initial estimate can then be refined using the secant-method recursion

$$\alpha_{n+1} = \alpha_n + \frac{(1 - \alpha_n)(\mathcal{A}_{N-1}^{\alpha_n NK} - \mathcal{I}_N^{\alpha_n NK})}{(\mathcal{A}_{N-1}^{\alpha_n NK} - \mathcal{I}_N^{\alpha_n NK}) - (\mathcal{A}_{N-1}^{NK} - \mathcal{I}_N^{NK})}. \qquad (44)$$

In practice, it is observed that only one or two iterations are sufficient to determine the value of the coefficient $\alpha^{NK} = \lim_{n \to \infty} \alpha_n$ and bring the difference $\mathcal{A}_{N-1}^{\alpha NK} - \mathcal{I}_N^{\alpha NK}$ below 0.2 eV.

Physically, the coefficient α^{NK} is directly related to the magnitude of orbital relaxation upon electron removal. Indeed, α^{NK} can be viewed as a screening coefficient whose value is close to 1 for weakly relaxing ionized systems (since E_N^{NK} is already piecewise linear in the absence of orbital relaxation) and is found to be small when relaxation is strong (see Sec. III A). The corrective factor α^{NK} introduced here is thus endowed with a clear physical interpretation.

As a final note, it should be emphasized that we have adopted here a simple picture of orbital relaxation through the coefficient α^{NK}, which can be viewed as a uniform and isotropic screening factor. More elaborate screening functions could be employed (at the price of computational complexity). Such accurate screening approaches provide promising extensions of the αNK method and represent an interesting subject for future studies.

F. Reference transition-state occupation

We now proceed to examine the influence of the reference occupation on the accuracy of calculated total electron removal energies. To this end, we compare the average of the αNK differential electron removal energies (that closely approximates the total ionization potential) of carbon for f_{ref} different from and equal to $\frac{1}{2}$ in Figs. 5(a) and 5(b), respectively. In the former case, the diagram indicates that the average

$$\frac{1}{2}(\mathcal{A}_{N-1}^{\alpha NK} + \mathcal{I}_N^{\alpha NK}) \approx I_N^{\alpha NK} \qquad (45)$$

deviates significantly from its LSD counterpart, whereas such deviations do not occur in the case $f_{ref} = \frac{1}{2}$. In fact, from Eqs. (2), (28), and (42), it can be shown that

$$I_N^{\alpha NK}(f_{ref}) \approx I_N^{LSD} - \alpha^{NK}\Pi_N^{u,LSD}(f_{ref}) \qquad (46)$$

(neglecting orbital reconfiguration). Then, substituting the (restricted) Slater's approximation[48]

$$\Delta E_{i\sigma}^{u,LSD} \approx -\epsilon_{i\sigma}^{u,LSD}\left(f_{i\sigma} = \frac{1}{2}\right) \qquad (47)$$

into the definition of the non-Koopmans energy contributions [Eq. (21)], one can demonstrate that

$$\Pi_N^{u,LSD}\left(f_{ref} = \frac{1}{2}\right) \approx 0 \qquad (48)$$

to arrive at the relation

$$I_N^{\alpha NK}\left(f_{ref} = \frac{1}{2}\right) \approx I_N^{LSD}. \qquad (49)$$

This result explains the accuracy of the αNK correction in predicting total electron removal energies with the reference occupation $f_{ref} = \frac{1}{2}$.

It should be noted that in the particular case of one-electron systems, $f_{ref} = \frac{1}{2}$ is not the only possible choice for the reference occupation. Indeed, due to the fact the Hartree and exchange-correlation potentials vanish for empty solitary orbitals, the approximation

$$\Delta E^{u,LSD} \approx -\epsilon^{u,LSD}(f = 0) \qquad (50)$$

also holds; hence, the solution $f_{ref} = 0$ is equally valid. In fact, for one-electron systems, $f_{ref} = 0$ leads to the exact one-electron Hamiltonian and the exact solution to the one-electron Schrödinger problem.

As an alternative to transition-state arguments, the value of f_{ref} can be justified by inspecting the sum rule satisfied by the exchange-correlation hole (xc hole).[10,51,52] The xc hole h_{xc} is defined by the relation

$$E_{xc} = \frac{1}{2}\int d\mathbf{r}d\mathbf{r}'\frac{\rho(\mathbf{r})h_{xc}(\mathbf{r},\mathbf{r}')}{|\mathbf{r}-\mathbf{r}'|} \qquad (51)$$

and can be explicitly written through the adiabatic connection formalism as

$$\rho(\mathbf{r})h_{xc}(\mathbf{r},\mathbf{r}') = \langle\hat{\rho}_2(\mathbf{r},\mathbf{r}')\rangle_\lambda - \rho(\mathbf{r})\rho(\mathbf{r}') \qquad (52)$$

with

$$\langle\hat{\rho}_2(\mathbf{r},\mathbf{r}')\rangle_\lambda = \int_0^1 d\lambda\langle\Psi_\lambda|\hat{\rho}_2(\mathbf{r},\mathbf{r}')|\Psi_\lambda\rangle. \qquad (53)$$

In Eq. (53), $\hat{\rho}_2(\mathbf{r},\mathbf{r}') = \hat{\psi}^\dagger(\mathbf{r})\hat{\psi}^\dagger(\mathbf{r}')\hat{\psi}(\mathbf{r}')\hat{\psi}(\mathbf{r})$ denotes the pair density operator and Ψ_λ stands for the ground state of a fictitious system where the Coulomb interaction is scaled down by λ and the effective local single-electron potential v_λ
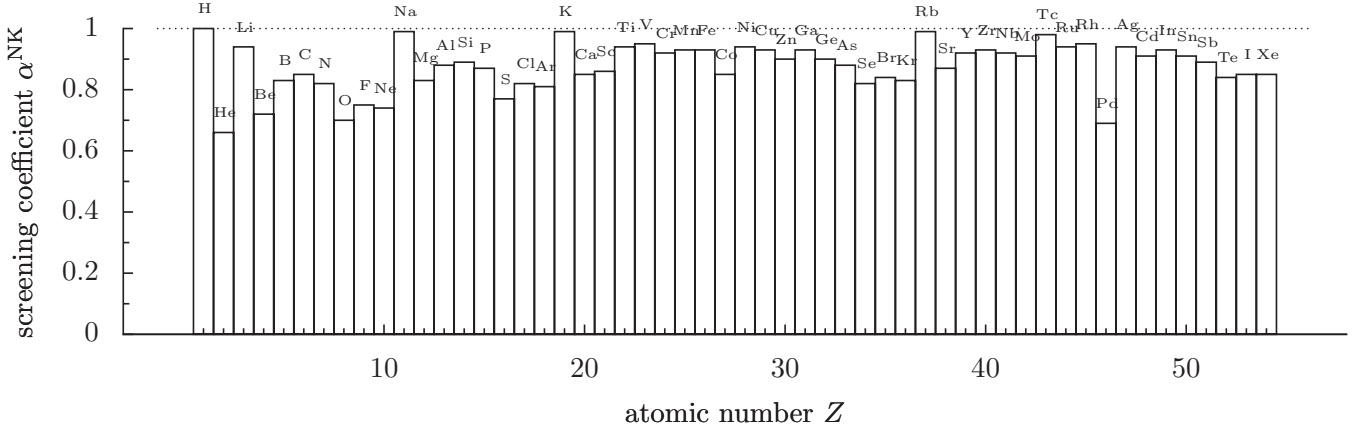
FIG. 6. Non-Koopmans screening coefficients α^{NK} for the elements of the five first periods.

is added to the Hamiltonian to keep the ground-state density constant with respect to λ.

By definition,[10,53] the exact xc hole corresponding to a system with a fractional number of electrons $N+\omega$, satisfies the sum rule

$$\int d\mathbf{r}' h_{\mathrm{xc}}(\mathbf{r},\mathbf{r}') = -1 + \omega(1-\omega) \int_0^1 d\lambda \frac{\rho_{\lambda,N+1}(\mathbf{r}) - \rho_{\lambda,N}(\mathbf{r})}{\rho(\mathbf{r})},$$
(54)

where the ground-state density $\rho_{\lambda,M}$ of the system with $M = N$ and $M = N+1$ electrons depends on λ due to the fact that M differs from $N+\omega$. It is important to note that the exact xc hole h_{xc} integrates to -1 only for integer electron numbers at variance with the LSD xc hole $h_{\mathrm{xc}}^{\mathrm{LSD}}$, which integrates to -1 irrespective of the number of electrons.

Turning now to the αNK xc hole $h_{\mathrm{xc}}^{\alpha\mathrm{NK}}$, it is possible to derive a relation similar to Eq. (54)

$$\int d\mathbf{r}' h_{\mathrm{xc}}^{\alpha\mathrm{NK}}(\mathbf{r},\mathbf{r}') = -1 + \alpha^{\mathrm{NK}} \sum_{i\sigma} f_{i\sigma}(2f_{\mathrm{ref}} - f_{i\sigma}) \frac{n_{i\sigma}(\mathbf{r})}{\rho(\mathbf{r})}$$
(55)

for $N \geq 1$ (the detailed derivation is presented in the Appendix). It is then clear that the occupation $f_{\mathrm{ref}} = \frac{1}{2}$ allows to satisfy the xc-hole sum rule exactly for integer number of electrons, and at least approximately for fractional numbers. (Note that in the case $N \leq 1$, the value $f_{\mathrm{ref}} = 0$ corresponds also to the exact sum rule.) For PZ, it has been argued that the enforcement of a similar sum rule is critical to the quality of the self-interaction correction.[44]

As a result, the explicit expression of the screened αNK functional with $f_{\mathrm{ref}} = \frac{1}{2}$ reads

$$E^{\alpha\mathrm{NK}} = E^{\mathrm{LSD}} + \alpha^{\mathrm{NK}} \sum_{i\sigma} \left[f_{i\sigma}(1-f_{i\sigma})E_{\mathrm{H}}[n_{i\sigma}] + E_{\mathrm{xc}}^{\mathrm{LSD}}[\rho - \rho_{i\sigma}] \right.$$

$$\left. + \int d\mathbf{r} v_{\mathrm{xc},\sigma}^{\mathrm{LSD}}\left(\mathbf{r}; \left[\rho + \left(\tfrac{1}{2} - f_{i\sigma}\right)n_{i\sigma}\right]\right)\rho_{i\sigma}(\mathbf{r}) - E_{\mathrm{xc}}^{\mathrm{LSD}}[\rho] \right].$$
(56)

In the next section, we assess the predictive accuracy of the

αNK functional given by Eq. (56), first focusing on atoms then extending applications to molecular systems.

III. APPLICATIONS

A. Atomic ionization

In order to probe the performance of the αNK functional, we calculate the electron removal energies of a complete range of atomic elements, from hydrogen to xenon, using the all-electron LD1 code of the QUANTUM-ESPRESSO distribution.[54] (Note that the atomic calculations that we report here do not account for relativistic effects; we have verified that the inclusion of scalar-relativistic contributions results in marginal deviations of <80 meV in the absolute precision of αNK differential electron removal energies.) The LD1 code proceeds by iterative integration of the spherically symmetric electronic-structure problem on logarithmic grids. The validity of this integration procedure, also employed by Perdew and Zunger in their original work,[10] has been extensively discussed and carefully verified by Goedecker and Umrigar.[41] More recently, Stengel and Spaldin have shown that the spherical approximation is actually required to prevent the appearance of unphysical hybrid states in the electronic structure of isolated atoms and predict physical atomic electron removal energies within orbital-dependent self-interaction corrections.[35]

We first compute the screening coefficient α^{NK} [Eqs. (43) and (44)] for the elements of the five first periodic rows based on the electronic configurations tabulated in Ref. 55 (with the exception of Ni for which we used the slightly unfavored $4s^1 3d^9$ configuration instead of $4s^2 3d^8$ that overestimates the experimental ionization potential by more than 1 eV). The calculated α^{NK} are reported in Fig. 6. The graph confirms that the screening coefficient varies in a narrow range. Not unexpectedly, the value of α^{NK} is found to be maximal for the elements whose outermost electronic shell contains a single electron, such as hydrogen for which $\alpha^{\mathrm{NK}} = 1$ and alkali metals, e.g., $\alpha^{\mathrm{NK}}(\mathrm{Na}) = 0.99$. In contrast, the coefficient α^{NK} saturates to low values for filled shell elements, namely, noble gases, e.g., $\alpha^{\mathrm{NK}}(\mathrm{He}) = 0.66$, alkaline earth metals, e.g., $\alpha^{\mathrm{NK}}(\mathrm{Be}) = 0.72$, and filled shell transition metals, e.g., $\alpha^{\mathrm{NK}}(\mathrm{Pd}) = 0.69$.
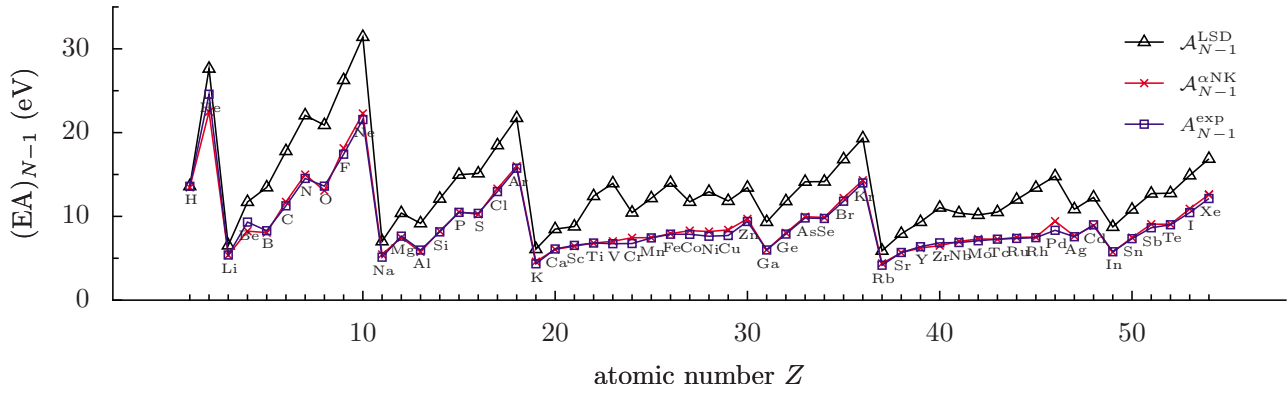
FIG. 7. (Color online) LSD and αNK differential electron affinities $\mathcal{A}_{N-1}$ (i.e., opposite energy of the lowest unoccupied orbital of the ionized atom X^+) compared with experiment for the elements of the five first periods.

After calculating atomic screening coefficients, we compare αNK differential electron affinity predictions with LSD and experiment in Fig. 7.[56] The comparison demonstrates the predictive ability of the αNK method, which brings partial electron removal energies $\mathcal{A}_{N-1}$ in very close agreement with experimental total electron removal energies A_{N-1}^{exp}, whereas LSD is found to considerably overestimate $\mathcal{A}_{N-1}$. In quantitative terms, the differential LSD energy $\mathcal{A}_{N-1}^{\mathrm{LSD}}$ is overestimated by more than 4 eV with a standard deviation of 1.85 eV [Fig. 8(a)]. Comparable deviations are obtained with the PZ self-interaction correction. The HF energy $\mathcal{A}_{N-1}^{\mathrm{HF}}$ are instead underestimated by a smaller margin of 1.48 eV. The αNK correction results in substantial improvement in the calculation of partial electron removal energies, reducing the error to 0.31 eV. Here, it is quite interesting to note that the αNK variational contributions counterbalance the slight tendency of the αNK$_0$ correction to underestimate electron removal energies within LSD.

We now examine partial ionization potential predictions (Fig. 9). A marked difference with the above electron affinity results is the enhanced accuracy of the HF and PZ theories. The improved performance in predicting atomic ionization potentials results from the fact that orbital relaxation compensates the absence of correlation contributions in HF and cancels residual non-Koopmans errors in PZ.[10] Nevertheless, even with beneficial error cancellation in favor of HF and PZ, the αNK deviation is still the lowest, approximately equal to the PZ mean absolute error of 0.34 eV [Fig. 8(b)].

The precision of αNK differential ionization energies reflects the intrinsic accuracy of the underlying LSD total energy functional in reproducing subtle atomic ionization trends that are difficult to describe with, e.g., semiempirical approximations.[40] To complement these observations, the full dependence of the LSD, PZ, and αNK relaxed energies ϵ_{2p} of the highest occupied atomic orbital of carbon as a function of its occupation is depicted in Fig. 10. Confronting the LSD and PZ graphs with those presented in Fig. 3, it is seen that orbital relaxation causes a non-negligible decrease in the unphysical shift $\epsilon_{2p}(1) - \epsilon_{2p}(0)$ of 1.5 eV for both functionals. Additionally, the PZ orbital energy $\epsilon_{2p}^{\mathrm{PZ}}$ becomes less curved at higher occupations, confirming that orbital relaxation enhances the performance of the PZ correction.[10] Nevertheless, the inflexion of the curve remains important in the

vicinity of $f_{2p}=0$ due to the fact that the PZ correction leaves the energy of the empty state almost unchanged. We observe that this unphysical trend is almost completely removed by the αNK correction, clearly showing that the screened αNK method is apt at imposing the generalized Koopmans' condition for any fractional value of f_{2p}.

The above comparisons demonstrate the predictive performance of the non-Koopmans method in correcting atomic

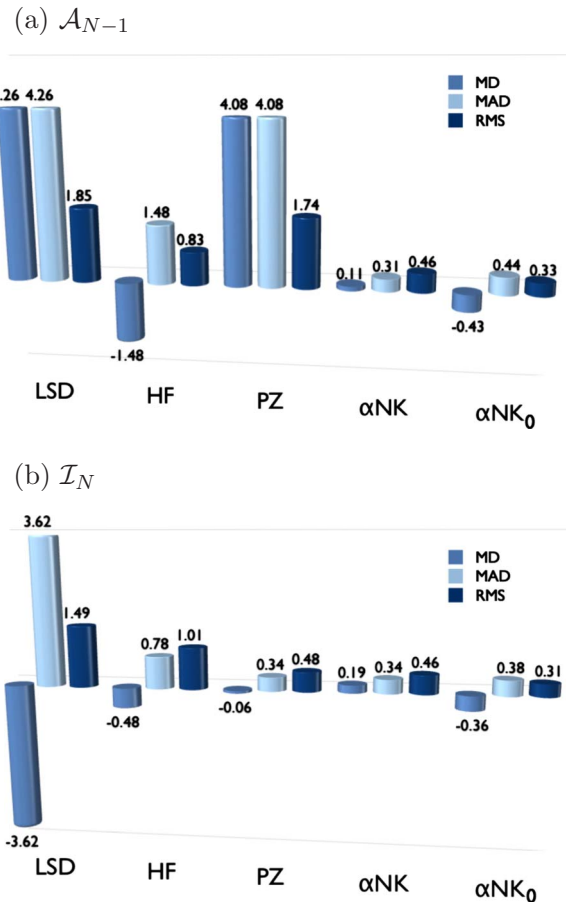(a) $\mathcal{A}_{N-1}$

(b) $\mathcal{I}_N$

FIG. 8. (Color online) *Atoms*: MD, MAD, and RMS deviations of LSD, HF, PZ, αNK, and αNK$_0$ atomic differential electron removal energies (a) $\mathcal{A}_{N-1}$ and (b) $\mathcal{I}_N$ relative to experiment for the elements of the five first periods. Energy errors are in eV.
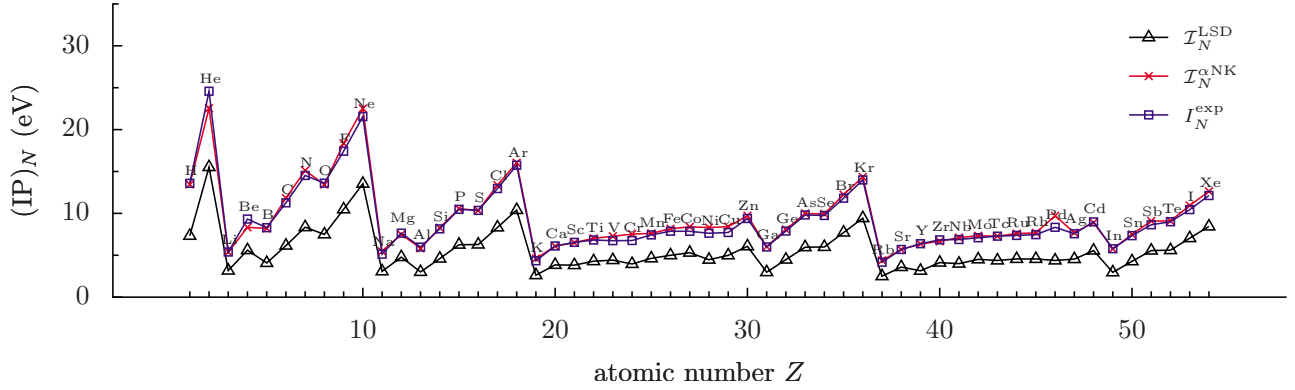
FIG. 9. (Color online) LSD and αNK differential ionization potentials $\mathcal{I}_N$ (i.e., opposite energy of the highest occupied orbital of the neutral atom X) compared with experiment for the elements of the five first periods.

differential electron affinities and first ionization potentials, placing $\mathcal{A}_{N-1}$ and $\mathcal{I}_N$ predictions on the same level of accuracy with respect to experiment. The fact that αNK improves $\mathcal{A}_{N-1}$ and $\mathcal{I}_N$ with the same precision ensures the accuracy of non-Koopmans total energy differences and related equilibrium properties. The results presented in the next sections provide further support to this conclusion.

B. Molecular ionization

In this section, we focus on the study of molecular systems. For this purpose, we have implemented the HF, PZ, and αNK methods in the plane-wave pseudopotential Car-Parrinello (CP) code of the QUANTUM-ESPRESSO distribution.[54] In this code, orbital optimization proceeds via fictitious Newtonian damped electronic dynamics.

The main difficulty in the CP implementation of the HF, PZ, and αNK functionals is the correction of periodic-image errors that arise from the use of the supercell approximation.[1] Such numerical errors preclude the accurate evaluation of exchange terms and orbital electrostatic potentials. To eliminate periodic-image errors in the plane-wave evaluation of exchange and electrostatic two-electron integrals, we employ countercharge correction techniques.[57] In addition to this difficulty, explicit orthogonality constraints must be considered for the accurate calculation of the gradient of the orbital-dependent PZ and αNK functionals.[41] To incorporate these

FIG. 10. LSD, PZ, and αNK relaxed orbital energies of the highest occupied state of carbon.

additional constraints, we use the efficient iterative orthogonalization cycle implemented in the original CP code.[58] In terms of computational performance, the cost of αNK calculations is here only 40% higher than that of PZ and lower than that of HF.

In Table I, we compare LSD, HF, PZ, and NK partial electron removal energy predictions for a representative set of molecules. In each case, molecular geometries are fully relaxed (the accuracy of equilibrium geometry predictions will be examined in Sec. III C). To perform our calculations, we employ LSD norm-conserving pseudopotentials[60] with an energy cutoff of 60 Ry for the plane-wave expansion of the electronic wave functions. With this calculation parameter, we verify that $\mathcal{A}_{N-1}$ and $\mathcal{I}_N$ are converged to within less than 50 meV.

It is frequently argued that substituting LSD pseudopotentials for their HF, PZ, and NK counterparts has minor effect on the predicted energy differences.[41] Comparing our pseudopotential calculations with all-electron atomic results (see Sec. III A), we actually found that the use of LSD pseudopotentials yields HF, PZ, and NK electron removal energies with a typical error of 0.1–0.2 eV. However, since these moderate deviations affect HF, PZ, and NK predictions in identical manner, the pseudopotential substitution does not alter the validity of the present comparative analysis.

As expected, one conspicuous feature in Table I is the poor performance of LSD that predicts molecular partial electron removal energies with an average error of ±40%. As was the case for atoms, the PZ self-interaction correction reduces the error in predicting $\mathcal{I}_N$ to less than 14%, which corresponds to an average deviation of 1.68 eV, whereas $\mathcal{A}_{N-1}$ predictions are not improved. In comparison, αNK partial ionization energies are predicted with a remarkable precision of 0.50 eV (4.1%) and 0.58 eV (4.8%) for $\mathcal{A}_{N-1}$ and $\mathcal{I}_N$, respectively. The αNK accuracy in predicting molecular vertical ionization energies compares favorably (arguably, even more accurately) with that of recently published fully self-consistent GW many-body perturbation theory calculations.[61]

It should also be noted that we perform here only one iteration [Eq. (43)] to determine the screening coefficient and that the calculated α^{NK} vary in a very limited range of values, even narrower than that found in the case of atoms (Fig.
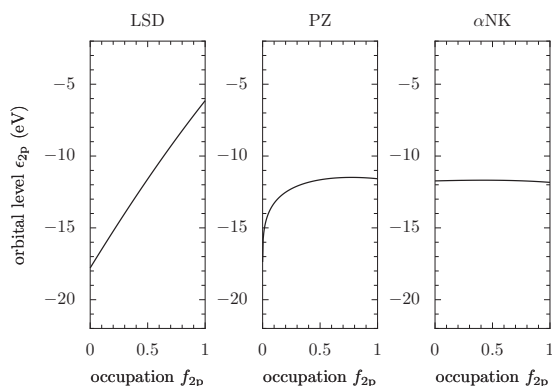
TABLE I. LSD, HF, PZ, αNK, and αNK$_0$ differential molecular electron removal energies compared with experimental vertical electron removal energies. Mean deviations (MD), mean absolute deviations (MAD), and root mean squared deviations of the error (RMS) in absolute and relative terms are also reported. The adiabatic ionization lower bound is given when the experimental vertical ionization energy is not available. Energies are in eV.

	LSD		HF		PZ		αNK		αNK$_0$		
	$\mathcal{A}_{N-1}$	$\mathcal{I}_N$	$\mathcal{A}_{N-1}$	$\mathcal{I}_N$	$\mathcal{A}_{N-1}$	$\mathcal{I}_N$	$\mathcal{A}_{N-1}$	$\mathcal{I}_N$	$\mathcal{A}_{N-1}$	$\mathcal{I}_N$	Expt.[a]
H$_2$	18.84	10.16	14.78	16.24	19.01	16.99	14.79	14.83	15.74	15.69	>15.43
N$_2$	20.85	10.37	12.77	17.15	21.55	17.78	16.14	16.20	15.38	15.52	>15.58
O$_2$	18.94	7.20	9.27	14.71	18.11	15.43	13.85	13.99	13.04	12.51	12.30
P$_2$	14.28	7.26	8.56	10.84	14.40	11.53	10.86	10.85	10.35	10.35	10.62
S$_2$	13.28	5.81	7.49	10.49	13.05	11.06	10.17	10.19	9.59	9.54	9.55
PH	13.92	5.81	8.39	10.25	13.81	10.84	9.94	10.02	9.68	9.68	>10.15
HCl	17.81	8.11	10.33	13.05	17.58	13.82	13.09	13.17	12.30	12.32	>12.75
CO	18.70	9.14	11.03	15.06	18.45	15.40	14.15	14.24	13.68	13.74	14.01
CS	15.20	7.42	7.30	12.83	14.53	13.29	11.63	11.76	10.83	10.89	>11.33
H$_2$O	18.97	7.33	8.97	13.81	18.50	14.77	13.17	13.45	11.75	11.94	>12.62
H$_2$S	14.87	6.39	8.17	10.55	14.70	11.52	10.77	10.86	10.15	10.17	10.50
NH$_3$	16.07	6.23	7.61	11.55	15.75	12.50	11.15	11.40	10.18	10.31	10.82
PH$_3$	14.50	6.84	8.29	10.46	14.15	11.45	10.77	10.83	10.41	10.41	10.59
CH$_4$	18.69	9.46	11.95	14.92	18.98	16.20	14.46	14.51	13.91	13.86	13.60
SiH$_4$	15.86	8.50	10.84	13.26	16.46	14.35	12.67	12.68	12.53	12.40	12.30
C$_2$H$_2$	16.19	7.40	8.79	11.40	16.19	12.97	12.05	12.14	11.11	11.15	11.49
C$_2$H$_4$	15.12	7.01	7.91	10.43	15.07	12.62	11.43	11.53	10.50	10.54	10.68
MD	4.57	−4.35	−2.46	0.75	4.47	1.66	0.40	0.49	−0.19	−0.19	
	38.5%	−36.4%	−21.0%	5.9%	37.4%	13.7%	3.4%	4.2%	−1.7%	−1.7%	
MAD	4.57	4.35	2.46	0.80	4.47	1.66	0.50	0.58	0.38	0.29	
	38.5%	36.4%	21.0%	6.4%	37.4%	13.7%	4.1%	4.8%	3.2%	2.5%	
RMS	0.95	0.63	0.83	0.73	0.89	0.66	0.46	0.48	0.40	0.28	
	7.7%	4.0%	7.4%	5.9%	6.3%	5.0%	3.7%	3.9%	3.3%	2.4%	

[a]Reference 59.

11). To conclude the analysis of $\mathcal{A}_{N-1}$ and $\mathcal{I}_N$ predictions, we focus on the influence of the variational contributions $\hat{w}_{\text{ref},i\sigma}^{\text{LSD}}$ and $\hat{w}_{\text{xd},i\sigma}^{\text{LSD}}$ on the accuracy of the αNK total energy method. Similarly to the comparative analysis presented in Sec. II D, we use the αNK$_0$ orbital-energy formulation to evaluate the magnitude of $\hat{w}_{\text{ref},i\sigma}^{\text{LSD}}$ and $\hat{w}_{\text{xd},i\sigma}^{\text{LSD}}$ errors. In agreement with the
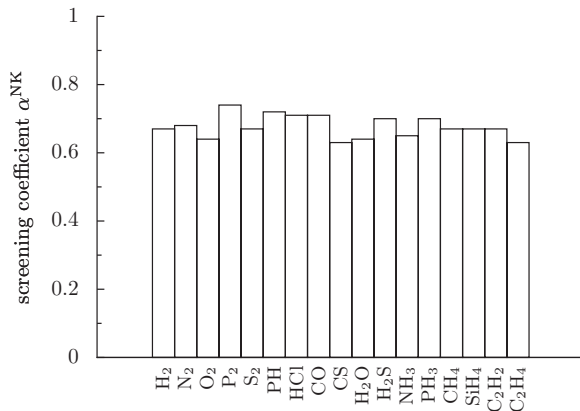

FIG. 11. Molecular non-Koopmans screening coefficients α^{NK}.

trend already observed, αNK$_0$ predictions for $\mathcal{A}_{N-1}$ and $\mathcal{I}_N$ are lower than αNK electron removal energies with negative shifts of 0.59 eV and 0.68 eV, respectively. (Thus, αNK$_0$ results are found to be even closer to experiment than their αNK counterparts with mean absolute error margins of only 3.2% for $\mathcal{A}_{N-1}$ and 2.5% for $\mathcal{I}_N$.) This direct comparison indicates that $\hat{w}_{\text{ref},i\sigma}^{\text{LSD}}$ and $\hat{w}_{\text{xd},i\sigma}^{\text{LSD}}$ introduce non-negligible energy shifts in the calculation of frontier orbital levels. However, these errors are much smaller than typical self-interaction deviations of 4–5 eV, providing quantitative justifications of the excellent precision of the αNK method.

C. Equilibrium structural properties

After analyzing partial electron removal energies, we now report on the accuracy of αNK equilibrium geometry calculations. We compare LSD, PZ, and αNK structural predictions to experimental bond lengths in Fig. 12 and we present LSD, HF, PZ, and αNK error bars in Fig. 13. The first important observation is the very good accuracy of LSD predictions with a mean absolute relative error of 1.1% for the seventeen molecules listed in Table I. PZ bond lengths are instead sensibly underestimated with a mean uncertainty of
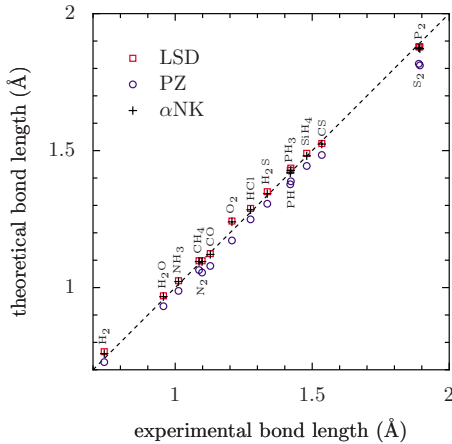
FIG. 12. (Color online) LSD, PZ, and αNK molecular bond lengths compared with experiment (Ref. 62).

2.8%. In contrast with PZ calculations, αNK results deviate from experiment by a relative error margin of 0.8%, which is lower than that of LSD, demonstrating that the αNK self-interaction correction does not deteriorate and even improves LSD structural predictions, at variance with the conventional PZ self-interaction correction.

These results illustrate the tendency of PZ to overbind molecular structures, and confirm the systematic improvement brought about by the αNK correction. The promising potential of the αNK correction in predicting other thermodynamical properties (e.g., dissociation energies and vibrational frequencies) will be critically explored in a separate study.

D. Photoemission energies

Having validated the non-Koopmans self-interaction correction for the calculation of electron removal energies and equilibrium structures, we now evaluate the performance of the αNK and αNK$_0$ methods in predicting photoemission energies, for which LSD and GGAs exhibit notable failures.
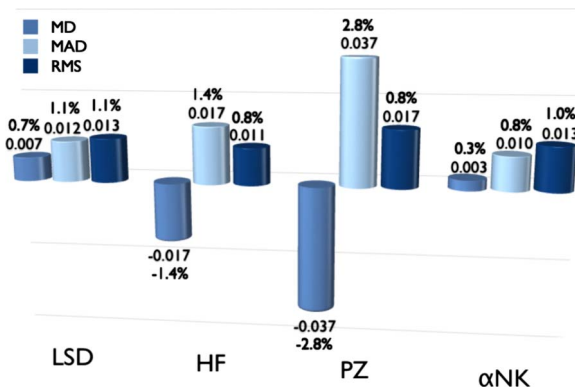

FIG. 13. (Color online) *Molecular geometries*: LSD, HF, PZ, and αNK MD, MAD, and RMS deviations of the error with respect to experiment of the predicted bond lengths for the 17 molecules listed in Table I. Error bars are in Å. Relative errors are also reported.

From the theoretical point of view, the very poor performance of LSD and GGA is expected; Kohn-Sham density-functional theory eigenvalues are not meant to predict excited-state properties.[63,64] In practice, total electron removal energies computed from constrained density-functional calculations (Δ_cSCF) are typically found to be in good agreement with experiment.[65,66] This level of accuracy suggests that orbital-dependent self-interaction corrected functionals can provide orbital energies in accordance with spectroscopic results.[67] This expectation is confirmed by PZ photoemission predictions for neon, argon, and krypton that we reproduce here using the LD1 code (Table II).

Nevertheless, similarly to the trend observed in Sec. III B, the predictive ability of PZ deteriorates in the case of molecular photoionization; this is at variance with the αNK method. To illustrate this fact, we compare LSD, HF, PZ, and non-Koopmans predictions for the photoemission spectrum (PES) of benzene in Table III and fullerene in Table IV. In the molecular photoemission calculations, we use the CP code with the computational procedure described in Sec. III B. We employ fully relaxed geometries for benzene and the LSD atomic structure of C_{60}, which is found to be in excellent agreement with the NMR experimental geometry.[70]

Focusing first on benzene, we observe that LSD underestimates electron binding energies with errors as large as 4.35 eV for low-lying states. In contrast to LSD, the HF theory provides overestimated photoemission energies with absolute deviations that increase gradually from 0.12 to 3.19 eV when approaching the bottom of the PES. Similar trends are observed for PZ with the difference that the errors do not systematically increase with increasing photoemission energies, leading in particular to the incorrect ordering of the e_{2g} and a_{2u} levels. In contrast, αNK restores the correct relative peak positions and yields slightly overestimated electron binding energies with an absolute precision of 4.9%. The slight tendency of αNK to overestimate electron binding energies is here again due to the influence of variational contributions, as directly confirmed by the performance of the αNK$_0$ orbital-energy method, which predicts photoemission energies in remarkable agreement with experiment.

Similarly to benzene, LSD energy predictions for fullerene are significantly underestimated. However, since the dispersion of the errors is much narrower than in the case of benzene, a simple shift of LSD photoemission bands, equal to the difference between the theoretical and experimental highest occupied molecular orbital levels, can bring the predicted PES in close agreement with experiment.[70] Despite the excellent precision of HF in the top region of the spectrum, HF photoemission energies are largely overestimated for low-lying states. In addition, HF inverts the h_g and g_g states in the second photoemission band although it predicts the correct peak ordering in the third and fourth bands.[65] The performance of PZ is found to be slightly worse than that of HF with significant qualitative errors in the grouping and ordering of the states. In contrast, αNK correctly shifts the spectrum and brings photoemission energies in very good agreement with experiment. Predicted αNK binding energies are also in excellent agreement with constrained LSD total energy differences,[65] providing a final validation of the performance of the αNK self-interaction

TABLE II. LSD, HF, PZ, and αNK orbital energies of neon, argon, and krypton compared with experimental photoemission energies. Relative MAD with respect to experimental photoionization results are also reported. The experimental photoemission energies of the spin-orbit doublets of p and d orbitals are indicated. Computational photoionization predictions do not include spin-orbit coupling. Energies are in eV.

		LSD	HF	PZ	αNK	Expt.[a]
Ne	$2p$	13.54	23.11	22.91	22.52	21.6–21.7
	$2s$	35.99	52.49	45.13	45.11	48.5
	$1s$	824.68	891.75	889.41	872.14	870.2
Ar	$3p$	10.40	16.05	15.76	16.04	15.7–15.9
	$3s$	24.03	34.74	30.22	30.54	29.3
	$2p$	229.77	260.45	256.12	254.65	248.4–250.6
	$2s$	293.73	335.30	315.49	315.40	326.3
	$1s$	3096.69	3227.47	3218.88	3193.55	3205.9
Kr	$4p$	9.43	14.25	13.97	14.35	14.1–14.2
	$4s$	22.33	31.34	27.78	28.27	27.5
	$3d$	83.65	104.06	101.29	101.67	93.8–95.0
	$3p$	192.84	226.70	209.04	210.71	214.4–222.2
	$3s$	253.48	295.21	269.48	271.24	292.8
	$2p$	1633.17	1714.53	1695.09	1692.46	1678.4–1730.9
	$2s$	1803.75	1902.11	1852.00	1853.32	1921.0
	$1s$	13877.37	14154.31	14128.17	14080.07	14326.0
MAD		19.2%	4.5%	3.3%	3.2%	

[a]Reference 62.

correction in bringing physical meaning to orbital energies—i.e., in identifying orbital energies as opposite total electron removal energies.

IV. SUMMARY AND OUTLOOK

In summary, we have demonstrated that the correction of the nonlinearity of the ground-state energy E_N as a function of the number of electrons N, at the origin of important discrepancies between total and differential electron removal energies, and related fundamental qualitative and quantitative self-interaction errors, can be achieved without altering the otherwise excellent performance of density-functional approximations in describing systems with nonfractional occupations. To construct the non-Koopmans self-interaction correction, we have first defined an exact non-Koopmans measure of self-interaction and adopted the frozen-orbital approximation (i.e., the framework of the restricted Koopmans' theorem) as a working alternative to the conventional one-electron paradigm. We have then accounted for orbital relaxation by introducing the screening coefficient α^{NK}, which bears the physical significance of a uniform and isotropic screening factor that can be determined iteratively—thereby closely satisfying the generalized Koopmans' condition. This self-interaction correction scheme can be applied to any lo-

TABLE III. LSD, HF, PZ, αNK, and αNK$_0$ orbital energies of benzene compared with experimental photoemission energies. Relative MAD with respect to experimental photoionization results are also reported. Energies are in eV.

	LSD	HF	PZ	αNK	αNK$_0$	Expt.[a]
e_{1g}	6.59	9.18	9.43	10.39	9.39	9.3
e_{2g}	8.28	13.54	15.46	12.66	12.48	11.8
a_{2u}	9.43	13.64	12.99	13.25	12.60	12.5
e_{1u}	10.33	16.02	17.67	14.75	14.56	14.0
b_{2u}	11.02	16.95	18.40	15.46	15.15	14.9
b_{1u}	11.26	17.51	18.82	15.65	15.69	15.5
a_{1g}	13.10	19.26	20.60	17.58	17.30	17.0
e_{2g}	14.85	22.39	22.72	19.27	19.34	19.2
MAD	26.1%	12.0%	18.4%	4.9%	2.1%	

[a]Reference 68.

TABLE IV. LSD, HF, PZ, and αNK orbital energies of fullerene C_{60} compared with constrained LSD total energy differences (Δ_cLSD) and experimental photoemission energy bands. Energies are in eV.

Band	LSD		HF		PZ		αNK		Δ_cLSD[a]		Expt.[b]
I	h_u	5.84	h_u	7.49	h_u	8.77	h_u	7.45	h_u	7.61	7.60
II	g_g	7.03	h_g	9.42	g_g	9.80	g_g	8.64	g_g	8.78	8.95
	h_g	7.15	g_g	9.64	h_g	10.48	h_g	8.75	h_g	8.90	
III	h_u	8.72	g_u	12.42	g_u	12.21	h_u	10.31	h_u	10.47	10.82–11.59
	g_u	8.74	t_u	12.99	t_u	12.69	g_u	10.35	g_u	10.50	
	h_g	9.03	h_u	13.08			h_g	10.64	h_g	10.79	
	t_u	9.28					t_u	10.91	t_u	11.03	
IV	g_u	10.05	h_g	13.46	h_u	14.13	g_u	11.66	g_u	11.79	12.43–13.82
	t_g	10.52	g_u	15.06	t_g	15.41	t_g	12.12	t_g	12.28	
	h_g	10.59	t_g	15.20	h_g	15.81	h_g	12.20	h_g	12.33	
			h_g	15.66							

[a]Reference 65.
[b]Reference 69.

cal, semilocal or hybrid density-functional approximation. The remarkable predictive performance of the non-Koopmans theory has been demonstrated for a range of atomic and molecular systems.

The theory developed here represents a significant step in the correction of electron self-interaction in electronic-structure theories. Nevertheless, interesting problems are left open. One central question is that similarly to the PZ approach, the αNK method leads to an orbital-dependent Hamiltonian, although it is always possible in principle to derive a consistent density-dependent formulation using, e.g., optimized effective potential mappings.[27] It is a long held tenet that the orbital dependence of self-interaction functionals and the subsequent loss of invariance with respect to unitary transformation of the one-body density matrix precludes applications to periodic systems (e.g., conjugate polymers and crystalline materials). In future studies, we will explore solutions to this central conceptual difficulty without resorting to density-dependent unitary invariant mappings.

APPENDIX: SCREENED NON-KOOPMANS EXCHANGE-CORRELATION HOLE SUM RULE

In this appendix, we derive the explicit expression of the αNK xc hole. Starting from the relation

$$E^{\alpha NK} = E^{LSD} + \alpha^{NK} \sum_{i\sigma} \left\{ E_{Hxc}^{LSD}[\rho - \rho_{i\sigma}] - E_{Hxc}^{LSD}[\rho] \right.$$
$$\left. + \int d\mathbf{r} \rho_{i\sigma}(\mathbf{r}) v_{Hxc,\sigma}^{LSD}(\mathbf{r}; [\rho_{i\sigma}^{ref}]) \right\} \quad (A1)$$

and from the definition of the xc hole [Eq. (51)], the contributions to the total αNK xc hole arising from the three summation terms in Eq. (A1) can be worked out. Those terms will be labeled $h_{xc,i\sigma}^{(a)}$, $h_{xc,i\sigma}^{(b)}$, and $h_{xc,i\sigma}^{(c)}$, respectively. Focusing on the first term, it is straightforward to obtain

$$h_{xc,i\sigma}^{(a)}(\mathbf{r},\mathbf{r}') = \frac{\rho(\mathbf{r}) - \rho_{i\sigma}(\mathbf{r})}{\rho(\mathbf{r})} [\rho(\mathbf{r}') - \rho_{i\sigma}(\mathbf{r}')]$$
$$+ \frac{\rho(\mathbf{r}) - \rho_{i\sigma}(\mathbf{r})}{\rho(\mathbf{r})} h_{xc}^{LSD}(\mathbf{r},\mathbf{r}'; [\rho - \rho_{i\sigma}]). \quad (A2)$$

Turning to the second term and including the appropriate sign, one obtains

$$h_{xc,i\sigma}^{(b)}(\mathbf{r},\mathbf{r}') = -\rho(\mathbf{r}') - h_{xc}^{LSD}(\mathbf{r},\mathbf{r}'; [\rho]). \quad (A3)$$

The third term is more complicated to derive since its expression is based on the exchange-correlation potential. Making use of the relation

$$v_{\text{xc},\sigma}(\mathbf{r};[\rho]) = \frac{1}{2} \int d\mathbf{r}' \frac{h_{\text{xc}}(\mathbf{r},\mathbf{r}';[\rho])}{|\mathbf{r}-\mathbf{r}'|}$$
$$+ \frac{1}{2} \int d\mathbf{r}' d\mathbf{r}'' \frac{\rho(\mathbf{r}')}{|\mathbf{r}'-\mathbf{r}''|} \frac{\delta h_{\text{xc}}(\mathbf{r}',\mathbf{r}'';[\rho])}{\delta \rho_\sigma(\mathbf{r})}$$

$$(A4)$$

the expression for $h^{(c)}_{\text{xc},i\sigma}$ becomes

$$h^{(c)}_{\text{xc},i\sigma}(\mathbf{r},\mathbf{r}') = \frac{2\rho_{i\sigma}(\mathbf{r})}{\rho(\mathbf{r})} \rho^{\text{ref}}_{i\sigma}(\mathbf{r}') + \frac{\rho_{i\sigma}(\mathbf{r})}{\rho(\mathbf{r})} h^{\text{LSD}}_{\text{xc}}(\mathbf{r},\mathbf{r}';[\rho^{\text{ref}}_{i\sigma}])$$
$$+ \frac{\rho^{\text{ref}}_{i\sigma}(\mathbf{r})}{\rho(\mathbf{r})} \int d\mathbf{r}'' \rho_{i\sigma}(\mathbf{r}'') \frac{\delta h^{\text{LSD}}_{\text{xc}}(\mathbf{r},\mathbf{r}';[\rho^{\text{ref}}_{i\sigma}])}{\delta \rho_\sigma(\mathbf{r}'')}.$$

$$(A5)$$

Regrouping all the terms, the expression for the exchange-correlation hole of the αNK functional can be written as

$$h^{\alpha\text{NK}}_{\text{xc}}(\mathbf{r},\mathbf{r}') = h^{\text{LSD}}_{\text{xc}}(\mathbf{r},\mathbf{r}';[\rho]) + \frac{\alpha^{\text{NK}}}{\rho(\mathbf{r})}$$

$$\times \sum_{i\sigma} \left\{ \rho^{\text{ref}}_{i\sigma}(\mathbf{r}) \int d\mathbf{r}'' \rho_{i\sigma}(\mathbf{r}'') \frac{\delta h^{\text{LSD}}_{\text{xc}}(\mathbf{r},\mathbf{r}';[\rho^{\text{ref}}_{i\sigma}])}{\delta \rho_\sigma(\mathbf{r}'')} \right.$$
$$+ f_{i\sigma}(2f_{\text{ref}} - f_{i\sigma}) n_{i\sigma}(\mathbf{r}) n_{i\sigma}(\mathbf{r}')$$
$$+ h^{\text{LSD}}_{\text{xc}}(\mathbf{r},\mathbf{r}';[\rho - \rho_{i\sigma}])(\rho(\mathbf{r}) - \rho_{i\sigma}(\mathbf{r}))$$
$$\left. - h^{\text{LSD}}_{\text{xc}}(\mathbf{r},\mathbf{r}';[\rho])\rho(\mathbf{r}) + h^{\text{LSD}}_{\text{xc}}(\mathbf{r},\mathbf{r}';[\rho^{\text{ref}}_{i\sigma}])\rho_{i\sigma}(\mathbf{r}) \right\}.$$

$$(A6)$$

The result given in Eq. (55) can be obtained from the above equation taking into account the xc-hole sum rule of the LSD functional, $\int d\mathbf{r}' h^{\text{LSD}}_{\text{xc}}(\mathbf{r},\mathbf{r}') = -1$ (valid for any electron number).

*daboi@cermics.enpc.fr

†Present address: Department of Materials, University of Oxford, Parks Road, Oxford OX1 3PH, United Kingdom.

[1] M. C. Payne, M. P. Teter, D. C. Allan, T. A. Arias, and J. D. Joannopoulos, Rev. Mod. Phys. **64**, 1045 (1992).

[2] R. G. Parr and W. Yang, *Density-Functional Theory of Atoms and Molecules* (Oxford University Press, Oxford, 1989).

[3] E. Goll, M. Ernst, F. Moegle-Hofacker, and H. Stoll, J. Chem. Phys. **130**, 234112 (2009).

[4] J. P. Perdew, R. G. Parr, M. Levy, and J. L. Balduz, Phys. Rev. Lett. **49**, 1691 (1982).

[5] R. G. Parr, R. A. Donnelly, M. Levy, and W. E. Palke, J. Chem. Phys. **68**, 3801 (1978).

[6] N. H. March and R. Pucci, J. Chem. Phys. **78**, 2480 (1983).

[7] W. Yang, R. G. Parr, and R. Pucci, J. Chem. Phys. **81**, 2862 (1984).

[8] J. P. Perdew and M. Levy, Phys. Rev. B **56**, 16021 (1997).

[9] R. S. Mulliken, J. Chem. Phys. **2**, 782 (1934).

[10] J. P. Perdew and A. Zunger, Phys. Rev. B **23**, 5048 (1981).

[11] A. J. Cohen, P. Mori-Sánchez, and W. Yang, Science **321**, 792 (2008).

[12] P. H.-L. Sit, M. Cocccioni, and N. Marzari, Phys. Rev. Lett. **97**, 028303 (2006).

[13] T. Stein, L. Kronik, and R. Baer, J. Am. Chem. Soc. **131**, 2818 (2009); U. Salzner, and R. Baer, J. Chem. Phys. **131**, 231101 (2009); T. Stein, L. Kronik, and R. Baer, J. Chem. Phys. **131**, 244119 (2009).

[14] C. Toher, A. Filippetti, S. Sanvito, and K. Burke, Phys. Rev. Lett. **95**, 146402 (2005).

[15] G. Kresse, A. Gil, and P. Sautet, Phys. Rev. B **68**, 073401 (2003).

[16] I. Dabo, A. Wieckowski, and N. Marzari, J. Am. Chem. Soc. **129**, 11045 (2007).

[17] H. J. Kulik, M. Cocccioni, D. A. Scherlis, and N. Marzari, Phys. Rev. Lett. **97**, 103001 (2006).

[18] P. Mori-Sánchez, A. J. Cohen, and W. Yang, J. Chem. Phys. **124**, 091102 (2006); E. R. Johnson, P. Mori-Sánchez, A. J. Cohen,

and W. Yang, J. Chem. Phys. **129**, 204112 (2008).

[19] O. A. Vydrov, G. E. Scuseria, and J. P. Perdew, J. Chem. Phys. **126**, 154109 (2007).

[20] S. Kümmel, L. Kronik, and J. P. Perdew, Phys. Rev. Lett. **93**, 213002 (2004).

[21] R. Baer and D. Neuhauser, Phys. Rev. Lett. **94**, 043002 (2005).

[22] P. Umari, A. J. Willamson, G. Galli, and N. Marzari, Phys. Rev. Lett. **95**, 207602 (2005).

[23] A. Ruzsinszky, J. P. Perdew, G. I. Csonka, G. E. Scuseria, and O. A. Vydrov, Phys. Rev. A **77**, 060502 (2008).

[24] J. P. Perdew and M. Levy, Phys. Rev. Lett. **51**, 1884 (1983).

[25] A. J. Cohen, P. Mori-Sánchez, and W. Yang, Phys. Rev. B **77**, 115123 (2008).

[26] P. Mori-Sánchez, A. J. Cohen, and W. Yang, Phys. Rev. Lett. **100**, 146401 (2008).

[27] S. Kümmel and L. Kronik, Rev. Mod. Phys. **80**, 3 (2008).

[28] A. J. Cohen, P. Mori-Sánchez, and W. Yang, J. Chem. Theory Comput. **5**, 786 (2009).

[29] A. Filippetti and N. A. Spaldin, Phys. Rev. B **67**, 125109 (2003).

[30] M. Cocccioni and S. de Gironcoli, Phys. Rev. B **71**, 035105 (2005).

[31] M. d'Avezac, M. Calandra, and F. Mauri, Phys. Rev. B **71**, 205210 (2005).

[32] A. Ruzsinszky, J. P. Perdew, G. I. Csonka, O. A. Vydrov, and G. E. Scuseria, J. Chem. Phys. **125**, 194112 (2006).

[33] V. I. Anisimov, A. V. Kozhevnikov, M. A. Korotin, A. V. Lukoyanov, and D. A. Khafizullin, J. Phys.: Condens. Matter **19**, 106206 (2007).

[34] L. G. Ferreira, M. Marques, and L. K. Teles, Phys. Rev. B **78**, 125116 (2008).

[35] M. Stengel and N. A. Spaldin, Phys. Rev. B **77**, 155106 (2008).

[36] S. Lany and A. Zunger, Phys. Rev. B **80**, 085202 (2009); **81**, 205209 (2010).

[37] R. A. Heaton, M. R. Pederson, and C. C. Lin, J. Chem. Phys. **86**, 258 (1987).

[38] V. L. Campo, Jr. and M. Cocccioni, J. Phys.: Condens. Matter **22**, 055602 (2010).

[39] F. Bruneval, Phys. Rev. Lett. **103**, 176403 (2009).

[40] R. Pucci and N. H. March, J. Chem. Phys. **76**, 6091 (1982).

[41] S. Goedecker and C. J. Umrigar, Phys. Rev. A **55**, 1765 (1997).

[42] O. A. Vydrov, G. E. Scuseria, J. P. Perdew, A. Ruzsinszky, and G. I. Csonka, J. Chem. Phys. **124**, 094108 (2006).

[43] O. A. Vydrov and G. E. Scuseria, J. Chem. Phys. **124**, 191101 (2006).

[44] A. Ruzsinszky, J. P. Perdew, G. I. Csonka, O. A. Vydrov, and G. E. Scuseria, J. Chem. Phys. **126**, 104102 (2007).

[45] J. F. Janak, Phys. Rev. B **18**, 7165 (1978).

[46] P. Mori-Sánchez, A. J. Cohen, and W. Yang, J. Chem. Phys. **125**, 201102 (2006).

[47] Our definition of the self-interaction energy $\Pi_{i\sigma}(f)$ differs slightly from that of Ref. 10 in that it is occupation-dependent and involves relaxed energies, thereby providing an exact measure of the curvature of the ground-state energy on the entire occupation segment $0 \leq f \leq 1$.

[48] J. C. Slater, *The Self-Consistent Field for Molecules and Solids: Quantum Theory of Molecules and Solids* (McGraw-Hill, New York, 1974), Vol. 4.

[49] I. Dabo, Ph.D. thesis, MIT (2007); I. Dabo, M. Cococcioni, and N. Marzari, arXiv:0901.2637 (unpublished).

[50] In deriving Eqs. (32) and (33), orbital occupations and squared wavefunctions must be written explicitly in terms of orbital densities as $f_{i\sigma} = \int d\mathbf{r}' \rho_{i\sigma}(\mathbf{r}')$ and $n_{i\sigma}(\mathbf{r}) = \rho_{i\sigma}(\mathbf{r}) / \int d\mathbf{r}' \rho_{i\sigma}(\mathbf{r}')$.

[51] D. C. Langreth and J. P. Perdew, Solid State Commun. **17**, 1425 (1975).

[52] O. Gunnarsson and B. I. Lundqvist, Phys. Rev. B **13**, 4274 (1976).

[53] P. Gori-Giorgi, J. G. Angyan, and A. Savin, Can. J. Chem. **87**, 1444 (2009).

[54] P. Giannozzi *et al.*, J. Phys.: Condens. Matter **21**, 395502 (2009).

[55] National Institute of Standards and Technology, *Physical Reference Data*, http://physics.nist.gov/

[56] Differential electron affinities can be directly calculated as the opposite energy of the lowest unoccupied orbital of the ionized atom since the derivative discontinuity contribution defined in Refs. 4 and 25 is absent for the LSD, HF, PZ, and non-Koopmans functionals.

[57] I. Dabo, B. Kozinsky, N. E. Singh-Miller, and N. Marzari, Phys. Rev. B **77**, 115139 (2008).

[58] K. Laasonen, A. Pasquarello, R. Car, C. Lee, and D. Vanderbilt, Phys. Rev. B **47**, 10142 (1993).

[59] National Institute of Standards and Technology, *Computational Chemistry Comparison and Benchmark Database*, http://cccbdb.nist.gov/

[60] W. E. Pickett, Comput. Phys. Rep. **9**, 115 (1989).

[61] C. Rostgaard, K. W. Jacobsen, and K. S. Thygesen, Phys. Rev. B **81**, 085103 (2010).

[62] *CRC Handbook of Chemistry and Physics* (CRC Press, Boca Raton, 2009).

[63] G. Onida, L. Reining, and A. Rubio, Rev. Mod. Phys. **74**, 601 (2002).

[64] M. Gatti, V. Olevano, L. Reining, and I. V. Tokatly, Phys. Rev. Lett. **99**, 057401 (2007).

[65] M. L. Tiago, P. R. C. Kent, R. Q. Hood, and F. A. Reboredo, J. Chem. Phys. **129**, 084311 (2008).

[66] P. R. T. Schipper, O. V. Gritsenko, S. J. A. van Gisbergen, and E. J. Baerends, J. Chem. Phys. **112**, 1344 (2000).

[67] D. P. Chong, O. V. Gritsenko, and E. J. Baerends, J. Chem. Phys. **116**, 1760 (2002).

[68] M. N. Piancastelli, M. K. Kelly, Y. Chang, J. T. McKinley, and G. Margaritondo, Phys. Rev. B **35**, 9218 (1987).

[69] D. L. Lichtenberger, K. W. Nebesny, C. D. Ray, D. R. Huffman, and L. D. Lamb, Chem. Phys. Lett. **176**, 203 (1991).

[70] B. P. Feuston, W. Andreoni, M. Parrinello, and E. Clementi, Phys. Rev. B **44**, 4056 (1991).